

**Title:**

Study of Vibrational Motions for Novel Compliant Needle used for Vibration-assisted Needle Insertion in Medical Applications

Authors:

Yi Cai, ycai@ncat.edu, North Carolina Agricultural and Technical State University

Jason Moore, jzm14@psu.edu, Pennsylvania State University

Yuan-Shin Lee, yslee@ncsu.edu, North Carolina State University

Keywords:

Vibratory Needle Insertion, Harmonic Analysis, Vibration Analysis, Biomedical Applications

DOI: 10.14733/cadconfP.2018.169-173

Introduction:

Needles are among the most widely used medical devices, and they serve in a wide variety of percutaneous procedures [3]. The effectiveness of a treatment and the success or precision of a diagnosis is highly dependent on the accuracy of percutaneous insertion [6]. Clinical studies have revealed that common factors that contribute to needle misplacement in percutaneous procedures include human errors imaging limitations, target uncertainty, tissue deformation and needle deflection [1, 2]. Among these factors, tissue deformation and needle bending are directly related to the forces experienced by the needle during the insertion procedure in a proportional manner [13]. Accordingly, a practical approach to reduce needle placement errors is to reduce the insertion force [7].

Among the efforts to reduce insertion force, vibratory needle insertion is a dynamic insertion technique where low-amplitude high-frequency vibration is applied to a needle in addition to the main insertion motion [4]. It has been demonstrated by researchers that it not only reduces the tissue cutting force at the needle tip, but also reduces the friction between needle shaft and tissue under certain conditions [4, 8-12]. A common limitation in the above research is that the dynamics of the vibrating needles was not studied systematically. A systematic study is needed for the dynamics of the needle vibration, so that the tip vibration mode of a needle can be determined, controlled and fine-tuned to be optimal for different insertion situations. Another limitation is that only needles with ordinary tip geometries were tested and only axial or transverse vibration was applied. It remains to be seen whether new needle tip design exists to better take advantage of vibration and whether a combination of axial and transverse vibration can further benefit.

This paper presents the vibration analysis of the novel compliant needle design proposed by the authors in [5] for vibration-assisted insertion in medical applications. The needle design is featured by its 4-bevel needle tip and micro-slots on the needle shaft. Harmonic analysis was applied to reveal the relationship between slot location and transverse vibration amplitude, which was later evaluated and validated by actual amplitude measurement of selected needle prototypes. Insertion experiment was also conducted to investigate how transverse vibration amplitude affect insertion force. This paper provides useful practical guidelines for design and optimization of needles for vibration-assisted insertion in medical applications.

Novel Compliant Needle for Vibration-assisted Insertion:

In our earlier works presented in [5], an innovative needle geometric design for vibration-assisted needles were developed for medical treatments. Fig. 1(a) shows the design of the medical needle for vibratory insertion. The needle tip is featured by the 4 bevels forming the needle tip and a micro slot on the shaft. The bevels are symmetrically distributed to form a spear shape. Among the four edges formed by the four bevels, the two associated the sharp corners of the spear shape are the main cutting edges during

Proceedings of CAD'18, Paris, France, July 9-11, 2018, 169-173

© 2018 CAD Solutions, LLC, <http://www.cad-conference.net>

needle insertion. The micro slot, where lies the major novelty of the proposed design, aims at modifying the stiffness symmetry of the needle and thus the frequency response. This design enables the main cutting edges to vibrate with high speed along both the Z and the X direction under axial stimulation at the base to perform micro tissue cutting, which will be beneficial to reduce the axial insertion force. An illustrative picture is shown in Fig. 1(b). The slot parameters include the number of slots, slot locations, depths and widths. It should be pointed out that the proposed needle is solid, so it can't be used like common hollow percutaneous needles for syringe injection. Instead, it will be used as the stylet section of the stylet/cannula combination widely used in biopsy and brachytherapy needles and trocars.

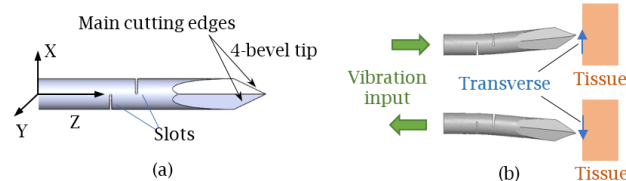


Fig. 1: The proposed needle design: (a) overview and (b) illustrative insertion.

Harmonic Analysis:

To study the effects of shaft slots on vibration modes, we began with the situation of one slot. The CAD models of 13 needles, namely N4 to N16, with one slot were built in SolidWorks where the distance between the tip and the slot changed from 4 mm to 16 mm with an interval of 1 mm. The needle length was set to be 60.9 mm, which was half wavelength of wave propagation in AISI 304 stainless steel at 40 kHz [5]. The slot width W was 100 μm , and the slot depth was $0.6D$, where D was the needle diameter being 1.27 mm (Gauge 18). For meshing of CAD models, the maximum element size was set to be 0.5 mm, the minimum was 0.05 mm. The minimum number of elements in a circle was 8, and the element size growth ratio was 1.5. The resultant number of nodes was 23987, and the number of elements was 14719. The maximum Jacobian Ratio was 3.47, the maximum aspect ratio of the elements was 4.43, and 99.5% of the elements had an aspect ratio lower than 3. All these parameters were under suitable ranges. Harmonic analysis was conducted to individual needle using an axial excitation with a peak-peak amplitude of 12.5 μm applied at the bottom of each needle between the frequencies of 38 kHz and 42 kHz. This amplitude was based on the capability of the available vibration device.

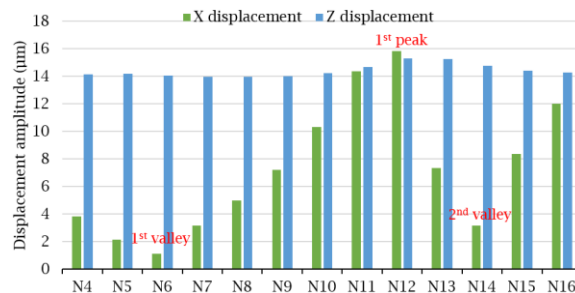


Fig. 2: Results of simulated X and Z displacement for N4 to N16 at 40 kHz.

For all the 13 needles, the X (transverse) and Z (axial) direction displacement of the needle tip were recorded. The displacement in the Y direction was at the magnitude of $10^{-1} \mu\text{m}$ and thus not recorded. Fig. 2 shows the results of X and Z displacement at the needle tip of N4 to N16 at 40 kHz. The Z displacements stay slightly higher than 12.5 μm among all the needles, which is the amplitude of excitation. It is interesting to notice that the X displacement changes in a period-like manner as the slot location changed from 4 mm to 16 mm. It reaches the peak value of 15.86 μm in N12, and valley values in N6 and N14. It is anticipated that another peak will appear after N16. The harmonic analysis also provided stress information on the needles. It was found that the maximum stress on a needle occurred at the bottom of the slot, and a larger transverse displacement at the needle tip was associated with a

Proceedings of CAD'18, Paris, France, July 9-11, 2018, 169-173

© 2018 CAD Solutions, LLC, <http://www.cad-conference.net>

larger value of maximum stress. Accordingly, N12 had the largest value of maximum stress among all the needles which was 166 MPa. Although this was below the yield strength of 304 stainless steel which is 215 MPa, fatigue analysis and optimization should be conducted in the future due to the cyclic loading.

Amplitude Measurement of Needle Prototypes:

Four needle prototypes with one slot, together with a control needle without slots, were fabricated with the dimensions shown in Tab. 1 using the EDM method presented in [5]. The four needles with slot were chosen based on Figure 7, where the X displacement at the needle tip increases from N6 to N12 and then decreases in N14. The displacements of the tips were measured using a Hirox KH-7700 3D Digital Microscope. Images were captured for each needle with and without vibration applied. The motion of the tip was determined by the ghost image in the capture. The motion can be tracked by measuring the displacement of the reflected spots caused by surface textures shown in Figure 3(a) and 3(b).

Needle	Length	φ	β	D	Slot-tip distance	H
N0(Control)	60.9 mm	10°	20°	1.27 mm	No slots	0.6D
N6					6 mm	
N9					9 mm	
N12					12 mm	
N14					14 mm	

Tab. 1: Summary of tested needle prototypes.

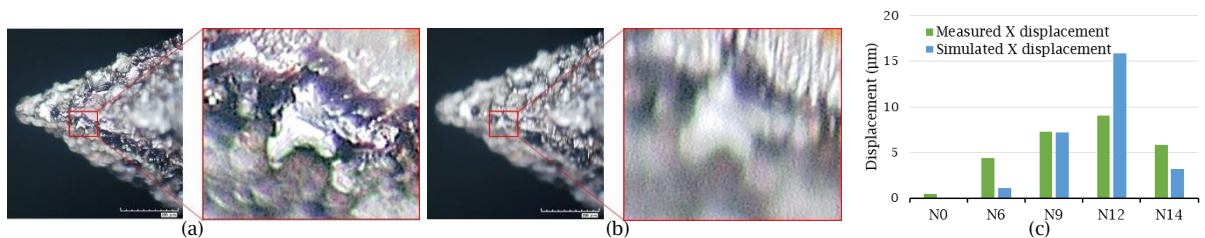


Fig. 3: Measurement of vibration amplitude using microscopic images: (a) without applied vibration, (b) with applied vibration, and (c) comparison with simulated results.

The results of measured X displacements are shown in Fig. 3(c) together with the harmonic analysis results extracted from earlier Fig. 2. The peak-peak motion amplitude at the end of the horn was measured to be 12.5 μm . Ideally, the control needle N0 should only have axial vibration. However, minor transverse vibration motion was still observed, which may be due to needle fabrication asymmetry. The needles with slot had motion in both the axial direction and the transverse direction. As the distance between the tip and slot increases from N6 to N12, the transverse displacement also increases, followed by a drop in N14. This follows the overall trend of the results of harmonic analysis in Fig. 2.

Vibration-assisted Insertion Experiment:

Fig. 4 shows the setup for the insertion experiment. A 50W 40 kHz ultrasonic transducer together with a horn was mounted to the slide on the linear motor to provide vibration during the tests. A strain gauge load cell (Lotoclub) of a capacity of 30 N was used to measure the force along the insertion direction, A data acquisition system (NI USB-6002) and LabVIEW software were used to record the force data. A polyurethane sheet (M-F Manufacturing) with a Shore Hardness of 40A and a thickness of 1.588 mm was used here as an analog to human skin. A rotational structure was used to hold the testing medium which was clamped by two plates with screws. The plates had 12 aligned holes in them. By rotating the plates together with the phantom, a needle can pass through the phantom at 12 different locations.

The five needles in Tab.1 were also used in this study. The control needle N0 was inserted with and without applied vibration, while each of the other four needles with slots was inserted with an applied axial ultrasonic vibration of 40 kHz, resulting in six needle-vibration combinations. Five trials were conducted for each combination. The average velocity of insertion was set to a constant of 2 mm/s for

all the trials, and the force data were collected for each trial with a sampling rate of 1000Hz. An example force-position plot is shown in Fig 5(a). Two parameters were measured as needle performance indicators. The first parameter is the puncture force, which is the peak value of insertion force before it suddenly drops. It is the maximum force the phantom endures before penetration begins. The second parameter is the friction force in the third phase. Keeping these two parameters low is usually preferred.

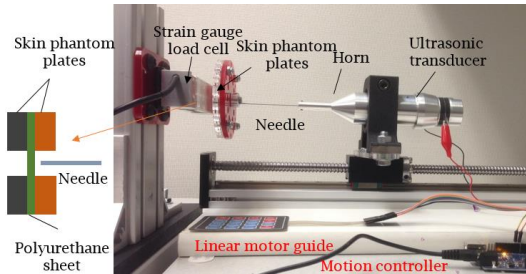


Fig. 4: Experiment setup for needle insertion with 40 kHz ultrasonic vibrator.

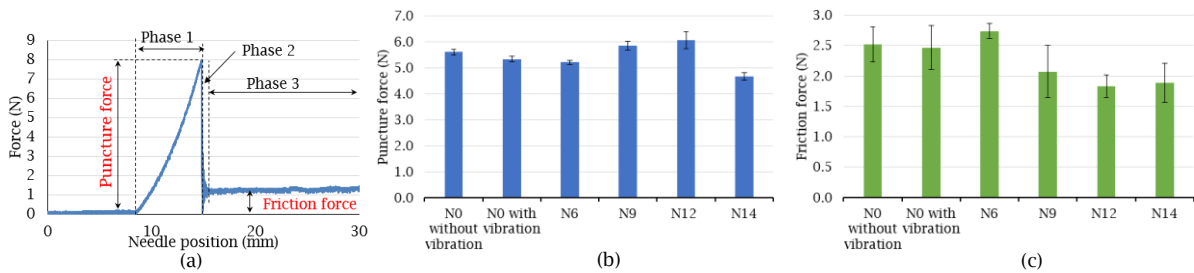


Fig. 5: Vibration-assisted insertion experiment: (a) example force-position plot, (b) results of puncture force, and (c) results of friction force.

The results are shown in Fig 5(b) and 5(c), respectively. Compared to the control insertion with no vibration, the puncture force was reduced with applied vibration by 4.98% for the control needle N0, and by 7.21% and 16.75% for N6 and N14, respectively. The ANOVA F -test p -values were 0.001, 0.001 and 0.001 respectively. On the other hand, the puncture force was increased by 4.36% and 8.09% for N9 and N12, respectively. The ANOVA F -test p -values were 0.013 and 0.010, respectively. N14 had the lowest mean value of puncture force, and it was tested to be significant. The friction force was reduced with applied vibration by 2.16%, 17.83%, 27.43% and 25.29% for N0, N9, N12 and N14, respectively. The ANOVA F -test p -values were 0.778, 0.060, 0.001 and 0.005, respectively. On the other hand, the friction force was increased by 8.58% for N6 with the ANOVA F -test p -value of 0.123. Although N12 had the lowest mean value of friction force, it was not significantly lower than that of N9 and N14 with ANOVA F -test p -values of 0.234 and 0.728, respectively.

By relating Fig. 5 and Fig. 3(c), it seems that a small amplitude of transverse vibration was helpful to further reduce the puncture force. As the amplitude increased, since the polyurethane film was relatively tough, the cutting edges of the needle were not able to cut a larger incision opening directly as expected. Instead, the increased transverse motion increased the transverse compressive force applied on the needle tip area, resulting higher resistant force. Moreover, the needle tip was not interacting with the testing medium with its best perpendicular orientation. Both reasons would increase the puncture force, so some needles like N9 and N12 even had larger puncture force with applied vibration than N0 without applied vibration. As the polyurethane film was finally penetrated with a larger puncture force, a larger area around the needle tip was affected and a larger incision opening was formed. This explained why the needles with larger puncture forces tended to have lower friction forces, just like the four needles with slots.

Conclusions:

This paper presented the vibration analysis of the design of novel compliant needle proposed by the authors in [5] for vibration-assisted insertion in medical applications. The results of harmonic analysis revealed that the transverse vibration amplitude changed in a periodic manner as the slot moved away from the tip, resulting several local amplitude peaks and valleys to choose from for different applications. The results of insertion experiment showed that axial vibration together with a proper level of transverse vibration ($6 \mu\text{m}$ in this case) gave the best effect in force reduction for the tested polyurethane material which mimicked human skin. This paper provides useful practical guidelines for design and optimization of needles for vibration-assisted insertion in medical applications.

Acknowledgements:

This work was supported by the NSF Grants (CMMI-1125872, CMMI-1404916 and CMMI-1547105) to North Carolina State University and the NSF Grant (CMMI-1404916) to The Penn State University.

References

- [1] Abolhassani, N.; Patel, R.; Ayazi, F.: Effects of different insertion methods on reducing needle deflection, Proceedings of the 29th IEEE Annual International Conference of EMBS, Lyon, France, 2007, 491-494. <http://dx.doi.org/10.1109/IEMBS.2007.4352330>
- [2] Abolhassani, N.; Patel, R.; Moallem, M.: Control of soft tissue deformation during robotic needle insertion, Minimally Invasive Therapy & Allied Technologies, 15(3), 2006, 165-176. <http://dx.doi.org/10.1080/13645700600771645>
- [3] Abolhassani, N.; Patel, R.; Moallem, M.: Needle insertion into soft tissue: A survey, Medical Engineering & Physics, 29(4), 2007, 413-431. <http://dx.doi.org/10.1016/j.medengphy.2006.07.003>
- [4] Barnett, A. C.; Jones, J. A.; Lee, Y.-S.; Moore, J. Z.: Compliant Needle Vibration Cutting of Soft Tissue, Journal of Manufacturing Science and Engineering, 138(11), 2016, 111011-111011. <http://dx.doi.org/10.1115/1.4033690>
- [5] Cai, Y.; Moore, J.; Lee, Y.-S.: Novel Surgical Needle Design and Manufacturing for Vibration-assisted Insertion in Medical Applications, Computer-Aided Design and Applications, 14(6), 2017, 1-11. <http://dx.doi.org/10.1080/16864360.2017.1287759>
- [6] DiMaio, S. P.; Salcudean, S. E.: Needle insertion modeling and simulation, IEEE Transactions on Robotics and Automation, 19(5), 2003, 864-875. <http://dx.doi.org/10.1109/TRA.2003.817044>
- [7] Han, P.; Kim, J.; Ehmann, K. F.; Cao, J.: Laser surface texturing of medical needles for friction control, International Journal of Mechatronics and Manufacturing Systems 1, 6(3), 2013, 215-228. <http://dx.doi.org/10.1504/IJMMS.2013.056449>
- [8] Huang, Y. C.; Tsai, M. C.; Lin, C. H.: A piezoelectric vibration-based syringe for reducing insertion force, IOP Conference Series: Materials Science and Engineering, 42(1), 2012, 012020. <http://dx.doi.org/10.1088/1757-899X/42/1/012020>
- [9] Kaiguo, Y.; Wan Sing, N.; Keck Voon, L.; Tien, I. L.; Yan, Y.; Podder, T.: High Frequency Translational Oscillation and Rotational Drilling of the Needle in Reducing Target Movement, Proceedings of IEEE International Symposium on CIRA Espoo, Finland, 2005, 163-168. <http://dx.doi.org/10.1109/cira.2005.1554271>
- [10] Khalaji, I.; Hadavand, M.; Asadian, A.; Patel, R. V.; Naish, M. D.: Analysis of needle-tissue friction during vibration-assisted needle insertion, Proceedings of IEEE/RSJ International Conference on Intelligent Robots and Systems (IROS), Tokyo, Japan, 2013, 4099-4104. <http://dx.doi.org/10.1109/IROS.2013.6696943>
- [11] Muralidharan, K., Mechanics of soft tissue penetration by a vibrating needle, M. S. thesis, University of Maryland, MD, United States, 2007.
- [12] Shin-Ei, T.; Yuyama, K.; Ujihara, M.; Mabuchi, K.: Reduction of insertion force of medical devices into biological tissues by vibration, Japanese journal of medical electronics and biological Engineering, 39(4), 2001, 292-296. <http://dx.doi.org/10.11239/jsmbe1963.39.292>
- [13] Wang, X.; Han, P.; Kang, M.; Ehmann, K.: Surface-blended texturing of medical needles for friction reduction using a picosecond laser, Applied Physics A, 122(4), 2016, 1-9. <http://dx.doi.org/10.1007/s00339-016-9892-2>